Human-like Interactive Behavior Generation for Autonomous Vehicles: A Bayesian Game-theoretic Approach with Turing Test

Yiran Zhang [1], Peng Hang[1], Chao Huang[1], and Chen Lv[1]

[1]Affiliation not available

October 21, 2021

Abstract

Interacting with surrounding road users is a key feature of vehicles and is critical for intelligence testing of autonomous vehicles. The Existing interaction modalities in autonomous vehicle simulation and testing are not sufficiently smart and can hardly reflect human-like behaviors in real world driving scenarios. To further improve the technology, in this work we present a novel hierarchical game-theoretical framework to represent naturalistic multi-modal interactions among road users in simulation and testing, which is then validated by the Turing test. Given that human drivers have no access to the complete information of the surrounding road users, the Bayesian game theory is utilized to model the decision-making process. Then, a probing behavior is generated by the proposed game theoretic model, and is further applied to control the vehicle via Markov chain. To validate the feasibility and effectiveness, the proposed method is tested through a series of experiments and compared with existing approaches. In addition, Turing tests are conducted to quantify the human-likeness of the proposed algorithm. The experiment results show that the proposed Bayesian game theoretic framework can effectively generate representative scenes of human-like decision-making during autonomous vehicle interactions, demonstrating its feasibility and effectiveness.

Corresponding author(s) Email: *lyuchen@ntu.edu.sg*

ToC Figure

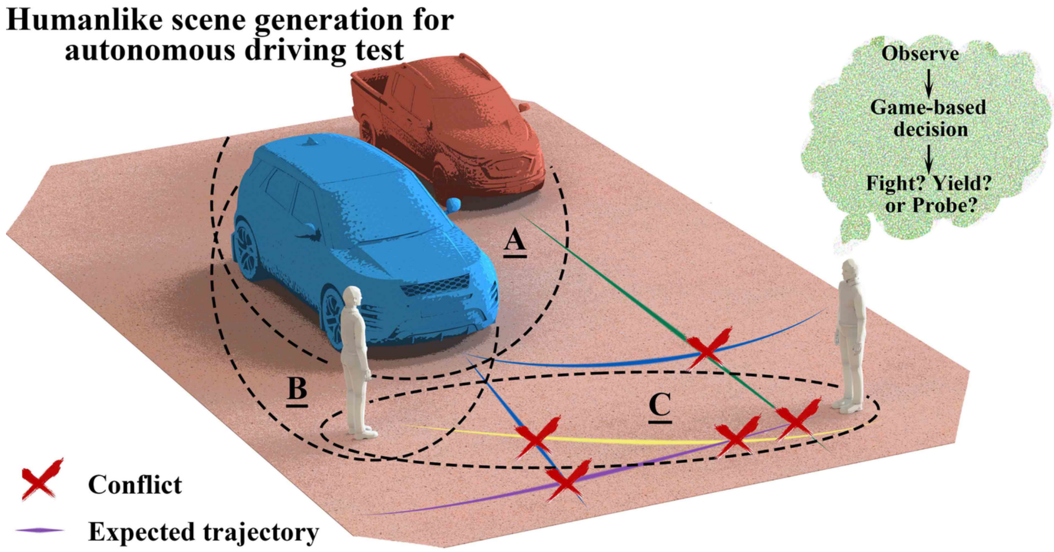

Figure 1: For the driving intelligence test, the road-users in the test scene should be interactive and humanlike. A generic approach is proposed inspired by referring to real human driver's behavior. First, the road users estimate the aggressiveness of the tested vehicle by observation. Then the observation is fed to the Bayesian game theoretic decision module. Based on the decision results, the road users can generate three different behaviors, to yield, to fight, and to probe.

Introduction

In the context of future smart mobility, there is an intensifying demand for naturalistic scene generation for automated vehicle simulation, intelligence testing and algorithm validation(Feng et al., 2021). The mixture of human-driven vehicles, pedestrians, and other intelligent autonomous agents will be on the roads, sharing the right of ways and interacting with one another, in the foreseeable future. In order to generate high-fidelity scenes for representing the new transportation modality, the interactive behaviors among heterogeneous traffic participants should be carefully considered. The conventional human-driven traffic participants, including pedestrians, cyclists, and human-driven cars, usually do not follow pre-defined trajectories or patterns, and their behaviors are difficult to predict in real world. But their decisions and actions are correlated, i.e. one's decision is made based on the constraints imposed by surrounding ones, and its behavior will also affect others in surround(Huang et al., 2021a; Yu et al., 2018; Hang et al., 2020a) . Besides, as a human has limited perception capability, the information one can obtain from the surrounding environment is limited (Dingus et al., 2016; Li and Busso, 2016; Kuo et al., 2019; Hu et al., 2021a). Further, their individual behaviors are usually highly personalized, as different road users have diverse travel demands, preferences and habits(Fridman et al., 2019; Martinez et al., 2018; Sama et al., 2020; Xing et al., 2020) . Thus, for the scene generation for autonomous driving, it is worthwhile exploring intelligent methods which can realize naturalistic and human-like interactive behaviors between intelligent agents. Instead of establishing comprehensive and large-scale various scenes, we focus on the intelligent representation of interacting moments. During interactions, the specific decision or intent of a road user is generally not available to the surrounding ones. However, through driving performance observation or driving style recognition, it is possible to infer their intents or possible actions using the trajectory prediction or aggressiveness estimation(Huang et al., 2021b), which is crucial in competing for the right of way. Moreover, one's aggressiveness or pattern my not always remain unchanged, as the situation and demand are varying, which makes the interactions game-like(Hang et al., 2020a, 2021b; Liniger and Lygeros, 2020) with incomplete information.

The understanding and modeling of interaction modalities among various road users, including cars, pedestrians, and cyclists, is critical, because information exchanges, time-varying reactions, and mutual influences would exert great impacts on the results of scene generation. Considering the above facts, in the context of human-like interactive scene generation for autonomous driving, challenges remain opening: What is the best strategy to win the right of road during interactions? And what is human's winning mechanism during interactions? To deal with the above problems, the decision logic behind the interaction with consideration of the aggressiveness should be explored first. Beyond this, the representation of human-likeness and its quantification method of human-likeness should be investigated as well.

To be more specific, we list some representative interactions and possible conflicts in **Figure** . The first situation is a vehicle-vehicle interaction, occurring during lane-change and merging. Besides, the vehicle-pedestrian interaction is also presented, and it is very important especially in unstructured or unsignalized areas. The third modality, i.e. the pedestrian-pedestrian interaction, which imposes more uncertainties to the autonomous driving scenarios, is included in the proposed paradigm as well. The most challenging situation is when road users conflict in their expected trajectories due to their non-cooperative behaviors. For instance, in the vehicle-pedestrian interaction case, the optimal solution for each of their trajectories (the yellow and blue lines, respectively, shown in Figure is to not decelerate. However, if both of them maintain their current speeds, a collision will be inevitable.

The Decision-making Behind the Scenes

Decision-making logics for autonomous vehicles and other road users can be similar and mutual-beneficial in terms of researches. Many scholars have studied the decision-making for autonomous vehicles(Kiran et al., 2021) and pedestrians(Kooij et al., 2016). Among them, learning-based approaches are promising and gaining popularity(Kiran et al., 2021). Some studies that human driving behaviors can be extracted through the machine learning algorithms, such as deep learning(Sama et al., 2020; Huang et al., 2020), imitation learning(Rehder et al., 2017), and inverse reinforcement learning(Sadigh et al., 2016). However, due to the inherent black-box nature of the neural networks, the interpret ability of learning based methods is not ideal. Inspired by the game-like essence of road users interactions, more interpretable game-theoretic approaches are investigated and considered more reasonable and practical. Some researches formulate the decision process as a Stackelberg game(Huang et al., 2021a; Yu et al., 2018; Hang et al., 2021b, 2020a) , and they impose a strong assumption on the availability of the leader as well as their utility function during the game. Furthermore, as the opponent vehicles may not always act as the formulated Stackelberg game expects, an online estimation algorithm is proposed using historical data to improve the game-based interactions (Zhang et al., 2020a) and(Zhang et al., 2020b) . Additionally, there exists a problem in finding Nash equilibrium. There may be more than one Nash equilibrium, thus they might conflict with one another(Wang et al., 2021; Spica et al., 2020) .

Apart from the above mentioned methods, MOBIL-IDM model has also been widely used and(Kesting et al., 2007) dominates the field of traffic scene generation. It is originally designed to be collision-free. However, after modifying some of the key parameters, such as the politeness, acceleration,and the grid distance estimation, the algorithm can generate adversarial behaviors for testing (Feng et al., 2021; Lindorfer et al., 2018). Other methods, including the risk field(Kolekar et al., 2020a), artificial potential field(Rasekhipour et al., 2017; Gao et al., 2019), constrained Delaunay triangulation(Huang et al., 2021b,a) , and scene prediction(Lawitzky et al., 2013), are capable of modeling human driver's cognitive states while considering safety. In general, the aforementioned methods either make strong assumptions on the availability of data and information, or lack integrity in representing human behaviors, resulting in in-ideal scenes for driving testing. Besides, being either adversarial or cautious, the generated behaviors of road users in the simulation testing should be human-like, to further improve the fidelity of the simulation testing environment. Moreover, currently both the learning-based and game-based approaches require heavy computation resources, which limit the implementation of advanced scene generation algorithms.

The Estimation of Driving Aggressiveness

Aggressiveness is an important factor for vehicles in the competition of right of ways(Huang et al., 2021b). It can be considered as a result of the trade-off between driving safety and travel efficiency(Zhang et al., 2020a). Due to the complexity of the problem, there is no unified method in measuring aggressiveness(Martinez et al., 2018). Intuitively, relative speed, acceleration, and the distance between vehicles can be utilized to quantify te aggressiveness(Huang et al., 2021b; Colombo et al., 2017; Li et al., 2019; Wang et al., 2017) . Nevertheless, using just vehicle dynamics to measure driving styles seems not very comprehensive. Thus, many studies shift to the driver-behavior oriented and scene-specific methods for the aggressiveness estimation(Solovey et al., 2014; Munir et al., 2020; Mole et al., 2021) . In recent years, some new elements are introduced to the discussions of the evaluation of aggressiveness. Many new explorations are conducted from the the aspect of scenes, e.g. straight road(Kolekar et al., 2020b)}, curves(Kolekar et al., 2020a), and roundabout(Hang et al., 2021a), as well as from the aspect of human factors — hand(Muhlbacher-Karrer et al., 2017), eye(Hu et al., 2021b), EEG(Rupp et al., 2019), and so forth.

However, these methods have two main drawbacks. First, the aggressiveness of a driver may not be consistent, due to the varying scenarios and the travel demands. Second, from the energy management perspective, although the driving style recognition is proved to be beneficial for long-term strategy optimization(Yang et al., 2018), obtaining the exact value of aggressiveness instantly may not be necessary. Therefore, instead of realizing an accurate and continuous value for the estimation, we maintain that an identification of the relative competitiveness or aggressiveness classification is a feasible and more pragmatic way for autonomous driving.

The Human-like Behaviors

One of the challenges that distinguish autonomous driving from other mobile platforms is the traffic uncertainty. From this point of view, representing human-like behaviors of road-users is very essential for scene generation. The results reported in(Feng et al., 2021) indicate that generating rare cases, i.e. using Markov model to randomly generate initial scenes and IDM-MOBIL model for adversarial behavior, can shorten the overall testing time. But the drawback is also clear. The Markov model is only used when the vehicle is cruising, thus there's no significant interactions between the ego vehicle and other surrounding ones. Besides, during the interactions, the IDM-MOBIL cannot completely represent human behaviors. Generating aggressive behaviors and possible accidents are essential, but these can be hardly realized if only non-human-like behaviors and interaction movements are produced in the simulation environment. Learning-based approaches are exploited as approximators for human-like driving as well(Li et al., 2018; Zhang et al., 2018). However, these methods suffer from the black-box nature of neural networks which can hardly be customized and interpreted for logic analysis. Learning from datasets is an interesting and promising methodology for realizing human-like driving (Xu et al., 2020), but the diversities and uncertainties of human driver behaviors should be further considered. Therefore, it is difficult to formulate all human decisions as a unified optimization problem, especially for solving a global optimum. And because human drivers have limited and various sensing and motor abilities, their control performances are imperfect.

Experimental Section/Methods

According to the aforementioned analysis, the formulated problem consists of two main elements: 1) Conflict. There will be a severe consequence if neither of the two interaction agents is willing to deviate from their original expected choices. Thus, one of them has to yield eventually. 2) Alternatives. Each of the participants should have at least two options, i.e. fight or yield. The conflict is defined as: the expected trajectories of multiple agents would cross. The expected motion trajectory is predicted based on an assumption of the current velocity and yaw angle. This is in line with the human-like concept, as a human does not make complicated and precise predictions (detailed definition is given in Note S2, Supporting Information). In this work, we will mainly focus on the alternatives.

Proposed Framework

The complete framework is shown in **Figure** 2 for interactive driving scene generation, which is explicit and inspired by the human's decision-making process. Within the framework, the scheduler is used to select players of interest. If any one is not selected, it will follow its own expected way-points, as how it moves has no direct impact on the driving situation of the tested vehicle. However, when one agent is selected, the candidate trajectory generator and algorithm in **Figure** 3 will be activated. The trajectory generator algorithm can be RRT (LaValle and Kuffner, 2001) , semi-reactive trajectory generation (Werling et al., 2010), and so forth as long as it can generate multiple possible trajectories for the player. Then, the algorithm will determine whether there exists a conflict between the expected trajectory and the prediction using the algorithm presented. If there is no conflict, the best solution will be selected from the candidates. If there exists a conflict, the algorithm will determine whether there is still available room to fight. If the ego player is not blocked, it will estimate the aggressiveness of other surrounding agents using the method proposed. Then, the aggressiveness will be updated for the decision-making module which is based on Bayesian game theory. If the decision is explicit, i.e. to fight or to yield, then the agent will follow the decision. However, when the decision is not clear, it will make some small steps for probing inspired from human behaviors. The small-step action is of low risk in terms of collision, but it is enough to demonstrate the agent's intention. This proposed framework is applicable for decision-making and interactions among multi-modal agents, including vehicles, cyclists and pedestrians, but in this work we will mainly focus on the interactions between vehicles.

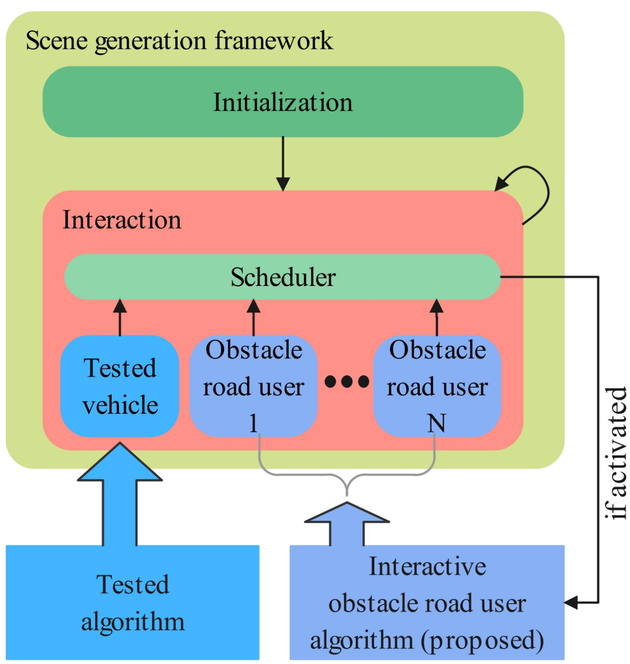

Figure 2: Scene generation framework

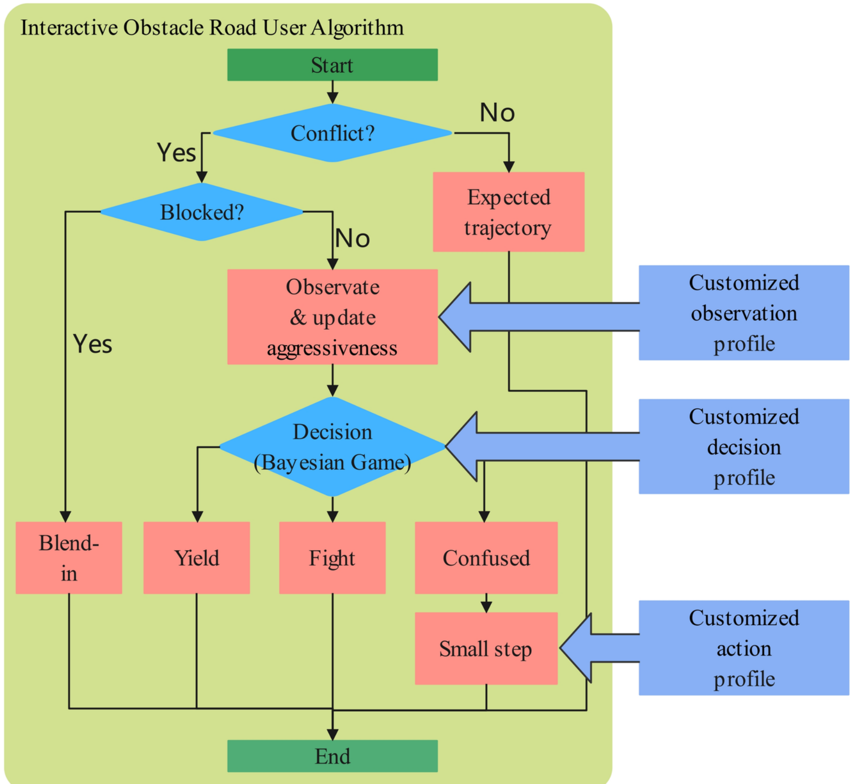

Figure 3: Framework of interactive scene generation algorithm

Bayesian Game Based Decision-making

Since the core algorithm for the interaction is the decision-making process, and the aggressiveness Observation & update module is designed to serve this process, we move the decision-making algorithm section forward though it is at the middle part of the proposed framework. This module is based on the Bayesian game theory which makes no assumptions on the accessibility of the cost function of the opponent or leader of the game. However, in order to simulate the subject for different scenes, cost function of the Player One is still required, which will be further formulated in the rest of this section.

Numerous scholars have studied game-theoretic approaches,in which an N-player game for $N = 2, 3, ..., n$ can be simplified into a two-player game, i.e., $N = 2$. For each player $i \in N$, he or she has at least two alternative solutions based on the problem definition represented by a discrete set of $A_i = \{a_{i,1}, a_{i,2}, \ldots, a_{i,k}, \ldots, a_{i,K}\}, K \in [2, \infty]$and the utility function given by $u_i(a_{i,k}, a_{i',k'})$. Based on the conflicts definition, A_i comprises two clusters of strategies, i.e. $A_i = \{A_{i,F}, A_{i,Y}\}$. $a_{i,F}(a_{i,F} \in A_{i,F})$, is the optimal or expected trajectory that maximize or minimize the utility function among all the alternatives to fight. And the mechanism is the same for the yielding type $a_{i,Y} \in A_{i,Y}$. Without loss of generality, the best solution always dominates the rest choices, thus it is not necessary to list all the choices.

Considering the lack of information of other agents, relative aggressiveness becomes important for decision making and interaction. Assuming the two players are player one and player two, from player one's perspective, the aggressiveness of player two can be classified into three types: equally aggressive, less aggressive, and more aggressive. The probability distribution of these three types $p_j(\sum p_j = 1(j = 1, 2, 3))$ subjects to a multinomial distribution. Different types of the player two have different forms of utility functions, which are summarized in **Table 1**.

Table 1: Decision model based on the Bayesian game theory

		Equally aggressive (p_1)		More aggressive (p_2)		Less aggressive (p_3)	
		Player Two		Player Two		Player Two	
		$a_{2,F}$	$a_{2,Y}$	$a_{2,F}$	$a_{2,Y}$	$a_{2,F}$	$a_{2,Y}$
Player One	$a_{1,F}$	(u_1, u_2)	(u_1, u_2)	(u_1', u_2)	(u_1, u_2)	(u_1, u_2')	(u_1, u_2)
	$a_{1,Y}$	(u_1, u_2)	(u_1, u_2)	(u_1, u_2)	(u_1, u_2)	(u_1, u_2)	(u_1, u_2)

For clarity, u_i is short for $u_i(a_{i,F/Y}, a_{i',Y/F})$. In the table, u_1' and u_2' refers to the more aggressive player's cost if she or he chooses to fight, which are supposed to be much smaller than u_i, because aggressive road-users tend to assume that there would be no collision. For simplification, we define that $u_1'(a_{1,F}, a_{2,Y}) = u_1(a_{1,F}, a_{2,Y})$and $u_2'(a_{1,F}, a_{2,Y}) = u_2(a_{1,F}, a_{2,Y})$. Meanwhile, if Player One chooses to yield, Player Two's choice (to yield or to fight) makes no difference to player one's cost, and vice versa. This means that $u_1(a_{1,Y}, a_{2,F}) = u_1(a_{1,Y}, a_{2,Y})$, $u_2(a_{1,Y}, a_{2,Y}) = u_2(a_{1,F}, a_{2,Y})$. To find the Bayesian Nash equilibrium, we have to extend the table using Note S3, Supporting Information. Let

$$\begin{cases} f_1(U_1, P) = sign(u_1(a_{1,Y}, a_{2,F}) - p_2 u_1(a_{1,F}, a_{2,Y}) - u1(a_{1,F}, a_{2,F})(p_1 + p_3)) \\ f_2(U_1, P) = sign(u_1(a_{1,Y}, a_{2,F}) - p_3 u_1(a_{1,F}, a_{2,F}) - u1(a_{1,F}, a_{2,Y})(p_1 + p_2)) \end{cases} \tag{1}$$

Under the following circumstances, (2) and (3), there will be only one equilibrium. Player one is confident to fight when

$$f_1(U_1, P) > 0, f_2(U_1, P) > 0 \tag{2}$$

Player one will choose to yield when

$$f_1(U_1, P) < 0, f_2(U_1, P) < 0 \tag{3}$$

However, player one will be confused if there is more than one equilibrium if

$$\begin{cases} f_1(U_1, P) < 0, f_2(U_1, P) > 0, or \\ f_1(U_1, P) > 0, f_2(U_1, P) < 0 \end{cases} \tag{4}$$

Notice that the final decision is defined by both probability and the cost function, for the vehicle-vehicle interactions, the cost function of the ego vehicle is given in Note S4, Supporting Information.

Aggressiveness Estimation and Belief Updating

The road-user's decision is based on her/his observation of the aggressiveness of the surrounding road-users. Aggressiveness is defined as a trade-off between safe distance and travel efficiency. Based on this definition, the observed aggressiveness is given by a sum of the longitudinal and lateral components, which aligns with the research of risk field: driver's reaction to the surrounding obstacles is a function of relative distance. Meanwhile, we also have to mitigate the part of distance variations that the subject driver generates. The risk field is simplified with the Gaussian model as in (5) where the parameters of the risk field can be obtained via the proposed experiments.

$$\alpha_{bv} = A_f(v, \Delta\varphi)\exp(-\frac{(x_{bv} - x_{sv} + v_{sv}\Delta t\cos(\varphi_{sv}))^2}{2\sigma_X^2(v_{sv})} - \frac{(y_{bv} - y_{sv} + v_{sv}\Delta t\sin(\varphi_{sv}))^2}{2\sigma_Y^2(\Delta\varphi_{sv})}) \tag{5}$$

where α_{bv} is the estimated aggressiveness of the obstacle vehicle. σ defines the shape of the aggressiveness field. The velocity in the numerator is to eliminate the variated distance created by the subject vehicle itself. In order to accurately measure the parameters, we first assume $A_f(\Delta v, \Delta\varphi)$, $\sigma_X(v_{sv})$, $\sigma_Y(\Delta\varphi_{sv})$ are linear as below.

$$\begin{cases} A_f(v_{sv}, \Delta\varphi) = \theta_1 v_{sv} + \theta_2\cos(\Delta\varphi) + \theta_3 \\ \sigma_X(v_{sv}) = \theta_4 v_{sv} + \theta_5 \\ \sigma_Y(\Delta\varphi_{sv}) = \theta_6\Delta\varphi + \theta_7 \end{cases} \tag{6}$$

Notice that the relative velocity is not included in (5) because according to the experiment questionnaires, drivers report that they usually are not able to estimate the relative velocity which can be, however, reflected in the distance variations.

After estimating the obstacle player's strategy, the subject player updates her/his belief about the driving style probability distribution, i.e., p_i in Table 1. The distribution of $\boldsymbol{p}$ *subjects to a Dirichlet distribution given by*

$$\begin{gathered} p(\boldsymbol{p}) \sim D(\beta_1, \ldots, \beta_K) = \frac{\Gamma(\sum_k \beta_k)}{\prod_k \Gamma(\beta_k)} \prod_k p_k^{\beta_k - 1} \\ where \quad p_k > 0 \\ \sum_k \boldsymbol{p}_k = 1 \end{gathered} \tag{7}$$

The algorithm updates hyper-parameters β_k based on the observation of the obstacle vehicle using (8).

$$\begin{cases} \beta_1^{t+1} = \beta_1^t + \kappa_1\left|\alpha_{bv} - \alpha_{sv}\right|, if\left|\alpha_{sv} - \alpha_{bv}\right| < \alpha_{th} \\ \beta_2^{t+1} = \beta_2^t + \kappa_2(\alpha_{sv} - \alpha_{bv}), if \alpha_{sv} - \alpha_{bv} \geq \alpha_{th} \\ \beta_3^{t+1} = \beta_3^t + \kappa_3(\alpha_{bv} - \alpha_{sv}), if \alpha_{bv} - \alpha_{sv} \geq \alpha_{th} \end{cases} \tag{8}$$

where α_{th} is the sensitivity threshold that the driver can spot. α_{sv}, α_{bv} are the aggressiveness of the subject vehicle and the background vehicle respectively. $\kappa_1, \kappa_2, \kappa_3$ are the sensitivity parameters. For the decision-making algorithm, the probability in (9) is replaced by the expectation of the Dirichlet distribution defined by

$$E\left[p_k\right] = \frac{\beta_k}{\sum_i \beta_i} \tag{9}$$

Experiment of aggressiveness estimation

In order to obtain the personalized parameters in (6), a series of experiments are conducted. All the experiments in this work are carried out using a 64-bit Windows 10 machine with an Intel Core i7 CPU, 32 GB of memory installed, and two Logitech G29 for driver input. The experiment environment is based on Simulink and Unreal engine with 10Hz sampling rate. Aggressiveness is an abstract idea and is difficult to quantify. Nevertheless, what we can obtain from the experiment is the extremity of aggressiveness, i.e., aggressiveness = 1. Hence, this experiment is designed to find the participant's limitations and then fit it into (6). In the experiment, the participant can observe the subject and surrounding vehicle, but she or he has no control over the subject vehicle except a stop button to terminate the experiment (details can be found in Note S8, Supporting Information). The subject vehicle and the obstacle vehicle initiated with a constant steering angle and velocity, which are designed to ensure a collision if the experiment is not stopped by the participant. The participant is asked to stop when she or he thinks the obstacle is too aggressive to undertake. When she or he stops, we record the current relative position and yaw angle. The subject vehicle is controlled by a PID controller with white Gaussian noise to enrich the dataset. After 5 repeated sets of experiments, the vehicle starts at a new position as in **Figure 4**. There are a total of 6 different angles for collision. After that, we change the speed for another set of experiments. The obstacle maintains constant velocity and yaw angle. There are a total of 5 different velocity references. The experiment results and the fitting algorithm can be found in Note S5, Supporting Information. Meanwhile, comparisons of fitting results can also be found in Note S5, Supporting Information.

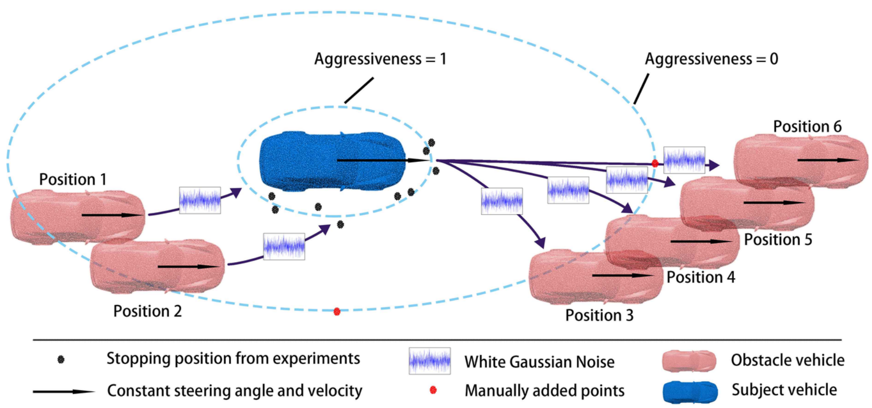

Figure 4: Diagram of proposed aggressiveness estimation method

Examples of the aggressiveness estimation function are given in **Figure 5**, **Figure 6**, **Figure 7**, **Figure 8**.

Probing Behavior Generation

If the subject vehicle is confused by the relative aggressiveness compared to the surrounding vehicles, it makes some small steps to test the real aggressiveness of the obstacle vehicles. These steps cannot be too big to trigger collisions, nor too small that shows no sign of his own intention. This part is what makes this work different from the extant studies. When dealing with uncertainties, current methods intends to give up or fight outright according to some fixed thresholds, such as time-to-collision. While, in reality, people intend to fight to certain degrees. If the obstacles are indeed more competitive, they will then eventually give up; but if not, they can win the right of way, especially during a traffic jam where human driver inclines to get to a more advantageous position. The small step is given by the algorithm in **Table 2**.

Figure 5: Case 1: velocity = 7m/s, relative yaw angle = 0 rad

rand is a random number generator between 0 and 1 to simulate randomness in reality for tests. The result of the above algorithm can be viewed as the subject vehicle's strategy or the aggressiveness that she or he wants to impose on the surrounding road users. However, this should be a value from 0 to 1, unconnected to the final control output. Hence, a Markov-based control strategy is proposed to build the connection. First, the Markov transition matrix based on one's driving habit is constructed based on experiments. The reason why insisting on experiments is that we can customize this matrix for different test applications. For example, we can collect different driving data from different drivers and abstract them into this matrix. When one special or random type of driving is required for the driving intelligence test. This matrix can

Figure 6: Case 2: velocity = 7m/s, relative yaw angle = pi/6 rad

be called for personalized behavior generating. We ask participants to repeat lane change under different driving speed 40 times and record their behaviors. For longitudinal control, the transitional probability to the next acceleration is given by the current velocity. For lateral control, the transitional matrix models the probability to the yaw angle increment based on the current velocity and current yaw angle. The results of a participant is reported in Note S6, Supporting Information.

Ideally, implanting the strategy interim α_{sv} into the Markov transitional probability is the best. However, as α_{sv} is an abstract variable, in order to connect the Small-Step strategy, the transitional probability above is not used directly. Inspired by (Shin and Sunwoo, 2019), the joint Markov chain is defined by

Figure 7: Case 3: velocity = 13 m/s, relative yaw angle = 0 rad

$$\pi_{a_{(i,j)}}^{t+1} = P(a_{t+1} = a_j \mid v_t = v_i)\mathcal{N}(2a_{gridX}(\alpha_{sv} - \alpha_M), \delta_x^2) \tag{10}$$

$$\pi_{s_{(i,j)}}^{t+1} = P(y'_{t+1} = a_j \mid v_t = v_i, \phi_t = \phi_i)\mathcal{N}(2a_{gridY}(\alpha_{sv} - \alpha_M), \delta_y^2) \tag{11}$$

These two equations can be viewed as a combination of behavior and strategy. $\mathcal N$ is a normal distribution with a mean of $2a_{gridX}(\alpha_{sv} - \alpha_M)$ or $2a_{gridY}(\alpha_{sv} - \alpha_M)$, and a standard deviation of δ_x or δ_y,

Figure 8: Case 4: velocity = 13m/s, relative yaw angle = pi/6 rad

which are tuned according to the grid distance of the Markov transitional matrix. α_M is given by the middle point of the transitional probability, which equals to 0.5 in this work. a_{gridX} and a_{gridY} are given by the shape of the transitional probability matrices. Ideally, the direction of fight or yield should be defined according to the gradient of risk-field (Kolekar et al., 2020a). To simplify, the direction of fight is given by the direction of shortening the distance of the two subjects, and the direction of yield is vice versa. The transitional probability we use are shown in **Figure 9**.

Table 2: Algorithm of a small step

SMALL_STEP($\alpha_{bv}, \alpha_{sv\_th}$)

if $\alpha_{bv} \leq \alpha_{sv\_th}$ **then**

$\alpha_{sv} \leftarrow \alpha_{sv\_last} + (\alpha_{sv\_th} - \max(\alpha_{bv}, \alpha_{sv\_last}))rand$;

else

$\alpha_{sv} \leftarrow \alpha_{sv\_last}(1 - rand)$;

end

$\alpha_{sv\_last} = \alpha_{sv}$;

Return α_{sv}

Experiment of the Turing Test

The experiment environment is given in **Figure** 11 and **Figure** 12. Two participants sits in two simulators separated by a barrier so that they can not see each other. The scene and parameters are also presented in Note S1, Supporting Information. Vehicle 1 can be manipulated by participant 2 or our algorithm. 20 rounds of tests were carried out. Male:16, Female:4, Driving license (M:4.56, SD:2.6977), Age (M:27.44, SD:2.56). The study protocol and consent form were approved by the Nanyang Technological University Institutional Review Board (protocol number IRB-2018-11-025).

The detailed procedure of the experiments are shown as below.

1) Before the test, we inform the participants the following items.

- The goal of the experiment is to distinguish (Driver B: V2) whether the opponent driver (Driver A: V1) is a human or an algorithm based on the interaction.
- The task of the scene as is depicted in Note S1, Supporting Information.
- The driver should follow the traffic rules.
- Their primary task should be the task of the scene: they should drive normally; the secondary task is the goal of the experiment: they can try to test vehicle 1. This is important because we think the driver should behave reasonably, but at the same time, it is necessary to give pressure to vehicle 1. When driving too cautious, without any conflict of interest, it is hard to evaluate the performance of vehicle 1. Also, the proposed algorithm is for scene generation. A human-like way to trigger an accident is sometimes needed.
- The driving style of the algorithm is randomly generated before each test.
- One single test takes 20 seconds and there will be a total of 10 tests for each participant

2) Two participants have few test rounds till they are familiar with the simulator and the dynamic performance of the vehicles. 3) After enough practice, driver B chooses to drive in autonomous mode or fully manual mode. If Driver B chooses autonomous mode. She or he also generates random driving style parameter (α_{th}). Driver A cannot see this process. 4) Driver B initiates one test and before the start of the test, Driver B informs Driver A so that Driver A can be well prepared for the experiment. 5) Complete one test. 6) Fill in a questionnaire. 7) Repeat step 3) to 6) nine more times. 8) score the entire experiment using Table in Note S7, Supporting Information. 9) After one set of tests, Driver B will be asked what is the criteria for their judgments.

The questionnaire for Driver A is only one question with five alternatives for each test (Question: rate the performance of Diver B. Choices: *Robot driver, Somewhat robot-like, Not sure, Somewhat human-like, Human driver*). The questionnaire for Driver B comprises 3 questions. (Question 1: the ground truth whether this test is driven by a human or an algorithm. Question 2: the driving style of Driver A. Choices: *Aggressive, Cautious, Normal.* Question 3: is there a collision in this test and which driver is responsible for

Figure 9: Longitudinal transitional probability (x: acceleartion(m/sˆ2), y: velocity (m/s), z: transitional probability (-))

the accidents?)

Figure 10: Lateral transitional probability (x: Velocity (m/s), y: ψ (degree), z: ψ'(degree/s), size: transitional probability (-)) ; The figure does not contain all the data because the original data size is large.

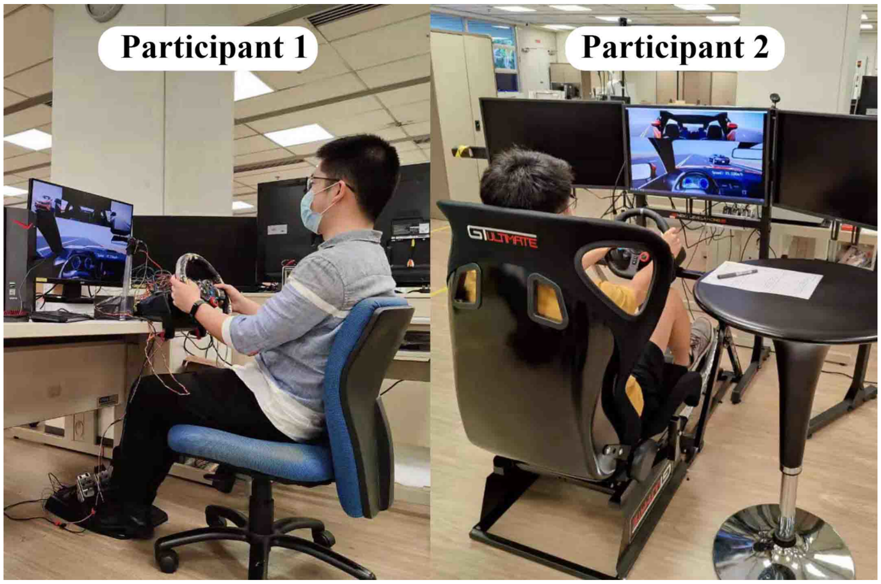

Figure 11: Turing test environment

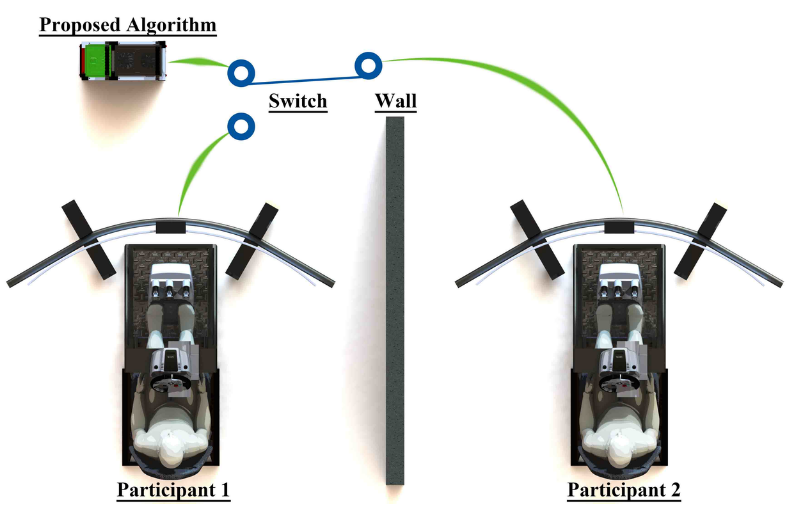

Figure 12: Turing test framework

Results

Three major results are reported in this section: the way to customize the driving behavior, the comparisons with existing methods, and the Turing test results.

Driving Behavior Customization

To demonstrate how the parameters in our algorithm will affect the interactive behavior, demonstrations are presented. The way to manipulate the driving behavior by adjusting α_{svth} and κ are reported and compared in this subsection. First, different thresholds α_{svth} are compared in **Figure ??**. For comparison, the surrounding vehicle (V1) stringently follows fixed predefined way-points, which, including other information, is unknown to the subject vehicle (V2) by setting the initiation $\beta_i^0 = \frac{1}{3}, i = i, 2, 3$. Also, the costs in Table 1 are set to a pair of constants for comparisons. Other parameters are given in Note S1, Supporting Information and (Werling et al., 2010) is used as the candidate trajectory generation algorithm.

Rich media available at https://www.youtube.com/watch?v=5tDlAgcQ_GA

Different κs are compared as well. Notice that we use different κs in (8), which is for different test requirements: some people might be more cautious under certain circumstances and reckless under others. For the comparison, we simplify the cases by assuming $\kappa = \kappa_1 = \kappa_2 = \kappa_3$.

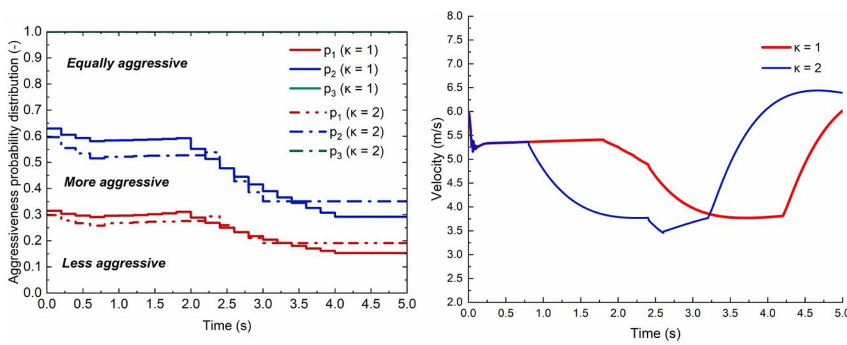

(a) Aggressiveness distribution comparison

(b) Velocity comparison

Figure 13: Customizing cautiousness

Comparisons with Existing Methods

To verify whether the proposed algorithm is reasonable and, furthermore, human-like, the algorithm is first compared with extant decision-making methodologies. In order to test the human-likeness, comparisons with researches that are proven to be human-like are conducted.

We compare our Bayesian game based approach with two widely accepted lane change decision-making methodologies: 1) IDM and MOBIL (metric 1a), which are the most frequently used method to imitate human driver's behavior as in **Figure** 14; 2) Xuemin's (Hu et al., 2018) method (metric 1b) , which uses a generates multiple alternatives and chooses one based on the cost function as in **Figure** 15.

To evaluate the human-likeness, the proposed method is compared to methods that are proven to be human-like. Pedestrian trajectories are generated using game theory as the first comparison in **Figure** 16 (metric 2a) . The two pedestrians' shortest trajectories to their respective goals are contradictory. Using the rapid random tree method with B-spline, multiple trajectories can be generated. The best trajectory in **Figure** 16

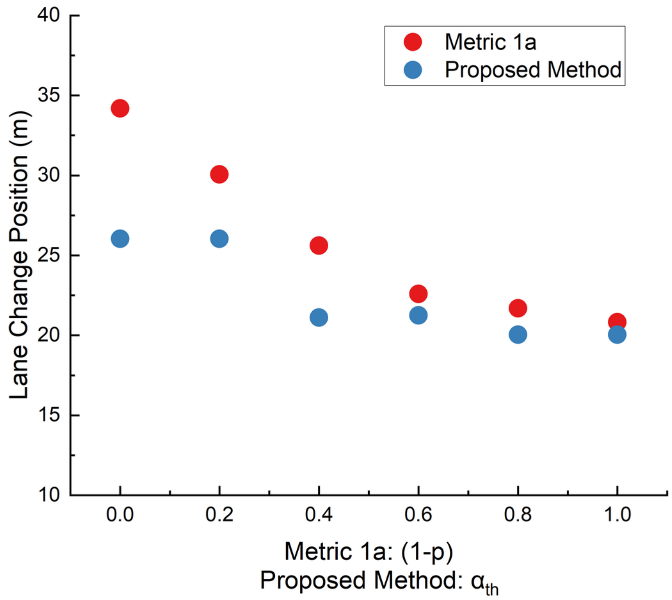

Figure 14: Comparison with IDM+MOBIL

Table 3: Turing test results

Range	Percentage
(8,10]	0%
(6,8]	30%
(4,6]	50%
(2,6]	20%
(0,2]	0%
Mean	5.2625
Standard deviation	1.6110

to fight is set to the shortest trajectory among all generated trajectories while the expected trajectory to yield is set to the shortest trajectoy without possible collision. Meanwhile, a comparison with game theoretic approach (Hang et al., 2020b) in Figure 17 (metric 2b) is also reported.

Turing Test

To verify the human-likeness of the proposed method, we conducted a Turing Test. The experiment results are summarized as in **Table** 3 and **Figure** 18. If the proposed algorithm is obviously different from human driving behavior, then the score should be close to 0 or 10.

Figure 15: Comparison with Xueming et.al's method (Blue: our method, Red: metric 2b method)

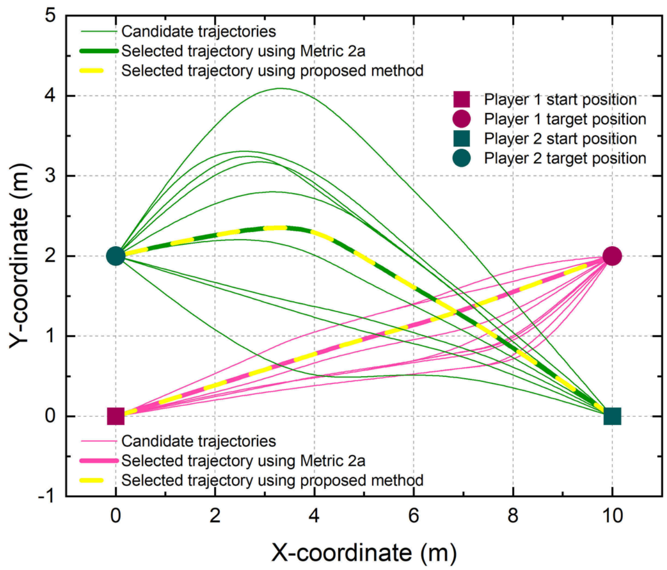

Figure 16: Comparison with Annemarie et.al's method

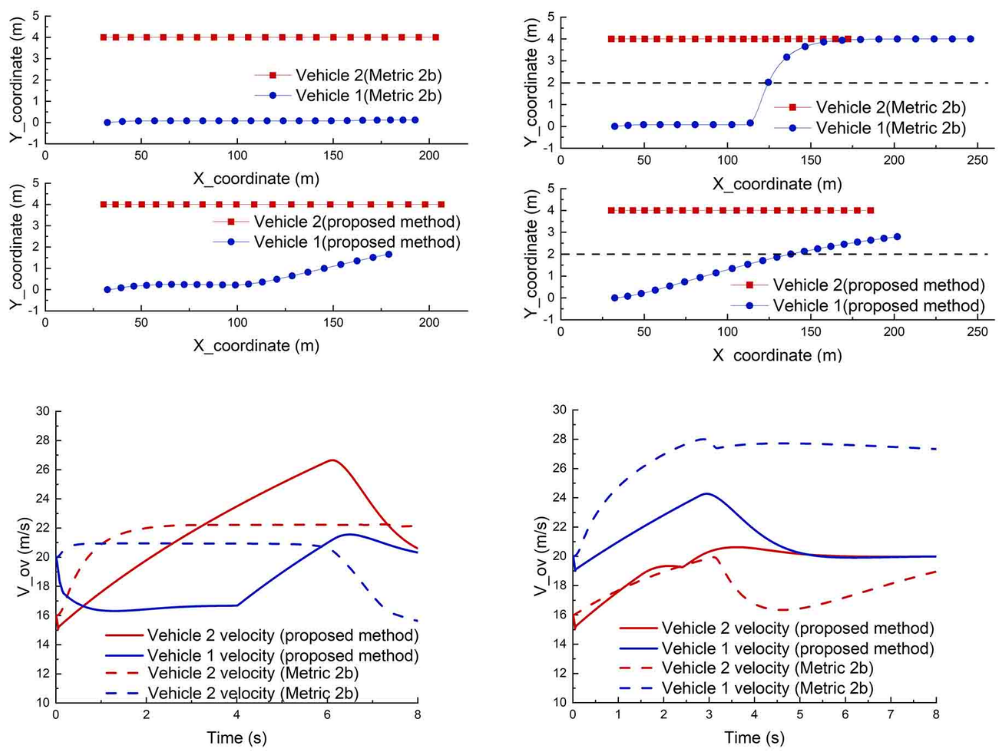

Figure 17: Comparison with Hang et.al's method

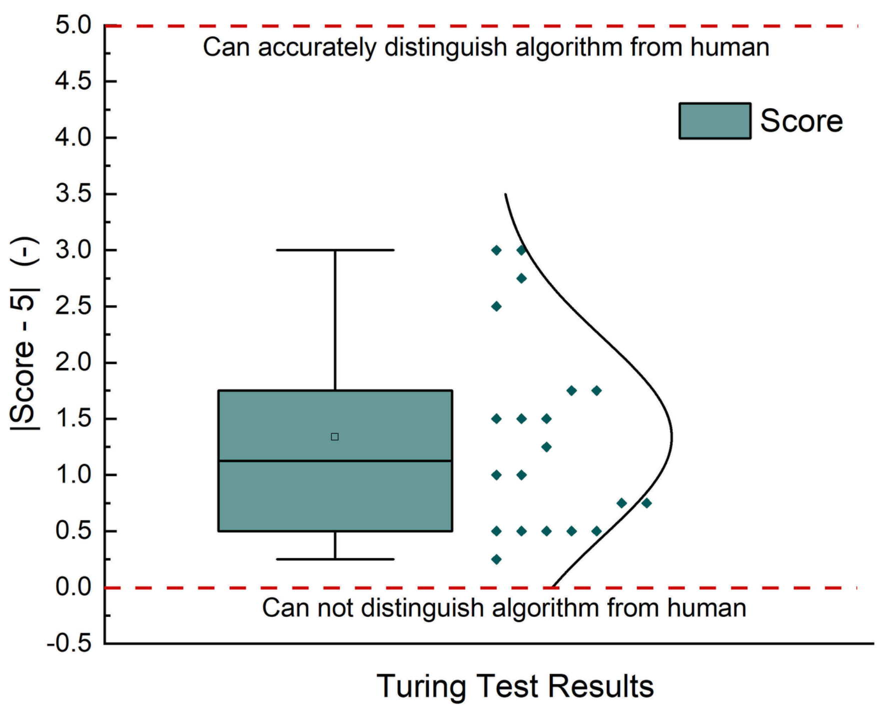

Figure 18: Turing test results

Four selected experiment video are shown in **Figure ??**.

Rich media available at https://youtu.be/SlhSdPmNHF0

Discussion

As can be seen in Figure **??**, all three cases start with a confusing situation because of the incomplete information assumption where V2 has no prior on V1. When $\alpha_{svth} = 0.5$, V2 believes that it is less aggressive than V1 as can be seen in Figure **??** (a) but it still accelerates a little bit to ensure this belief. After a short period of acceleration, it finds out that it is actually less aggressive, thus it decelerates to give the right of way as can be seen in Figure **??** (d) . On the other hand, when $\alpha_{svth} = 0.7$, V2 believes it is more aggressive than V1, as can be found in Figure **??** (b) , where the green region is the largest at the beginning. It accelerates longer to demonstrate its will to fight. After a turning point at around 3s, the subject vehicle doubts itself whether it is really more aggressive than the surrounding one. Because the obstacle vehicle follows pre-defined way-points no matter what happens, which can be seen as extremely aggressive. V2 yields eventually till there is no driving conflicts. However, when $\alpha_{svth} = 0.9$, V2 thinks it is more aggressive than the surrounding one. Thus it accelerates intensively, along with its belief as the green block in Figure **??** (c). After a short period of probing, it chooses to fight. Though, for the same reason, the obstacle vehicle can be seen as extremely aggressive. V2 doubts itself even it is driving parallel with the obstacle one. After a while, it knows that it is less aggressive, thus accelerates to get out of the situation. In this case, V2 is not more aggressive than the obstacle, but when the subject vehicle tries to probe, it accelerates more and finally blocked the surrounding road user.

As is shown in Figure 13, when $\kappa = 1$, the driver does not make a rush decision as compared to $\kappa = 2$: the relative aggressiveness varies less intensively. By tuning those above white-box parameters, various complex behaviors can be generated.

As in Figure 14, when the ego vehicle is less polite or more aggressive as defined in this paper, the driver intends to start a lane change earlier. However, our method are not exactly monotonous. This is because when the vehicle is probing, there are chances that the subject misjudged the obstacle vehicle's intention and also, the subject vehicle can block the obstacle vehicle, thus the obstacle vehicle has to yield. This means the proposed concurs with MOBIL's method, which is proved effective in modeling large traffic flow, while our method can generate micro and more complicated human behavior. Also, the comparison with Xuemin's(Hu et al., 2018) method in Figure 15 indicates that our method could be more aggressive. As can be seen in the early phase of lane change, the compared method is more conservative because, when there is a conflict of interest, the subject vehicle will choose a less costly candidate trajectory without conflict. However, the proposed method is adversarial because the algorithm assumes that the obstacle driver will yield eventually.

When we set the collision weight to infinite, the trajectories selected by the algorithm are the same as the compared method as is validated in Figure 16. It does not matter what P is because, when the collision cost is too high, our method will always choose a conservative alternative, which aligns with the literature.

Also, the comparison with Hang et.al's method . Figure 17b, vehicle 2 is assumed to be an aggressive driver. In our case, $\alpha_{th,v1} = 0.1$, $\alpha_{th,v2} = 1$ both methods indicate that the subject vehicle maintains a relatively low velocity. But there are two major differences. In Table Figure 17d, the subject vehicle of Hang et.al's method accelerates and maintains its speed at around 21m/s. However, to enlarge the space for lane-change, our vehicle 1 decelerates and then starts to accelerate at 5s to restart a lane-change. As can be seen, our method outperforms in lane changing time: proactive decelerating increases grid distance for a faster lane change. As for driver 2's behavior, though Hang's method accelerates intensively and maintains at around 22 m/s, our vehicle 2 does not accelerate much because vehicle 1 is faster, as can be seen as more aggressive, from 0s to 1s. Though the aggressiveness threshold of our vehicle 2 is 1, it accelerates conservatively to ensure driver 1's aggressiveness. Though from 4s to 8s, our method accelerates to a relatively high velocity to get rid of the lane-changing vehicle. The other situation is the opposite of case one. As can be found in Table Figure 17c and Figure 17e, vehicle 1 is quite sure that it is more aggressive, thus it starts a lane change at the early phase and accelerates to 24m/s at 3s. However, vehicle 2 does not quit fighting from 0s to 1s. The above phenomenon aligns with Hang's method, though from 3s to 8s, the two methods are different because, in the scene generation context, after the interaction, the vehicles are enforced to bounce back to the initial velocity, through which we can eliminate the chance of collisions with irrelevant vehicles, which can be tuned to Hang's method easily. Additionally, although the trends in the two methods are identical, the velocity or trajectories are not exactly the same. This is partially because Hang et.al use MPC for the control of vehicle which is a strong assumption because human drivers can control the vehicle perfectly.

According to the above comparisons, we can see, from the decision level, the proposed method concurs with the state of art literature and is more flexible and intelligent with respect to scene generation. Though, we compare the proposed method with some methodologies that are proven to be human-like, to further evaluate the human-likeness of this method, a variation of the Turing test is conducted.

In the Turing test, most people are not able to distinguish whether it is human or algorithm as 50% of them have approximately 50% accuracy. Also, the other participant's scores are closed to 50% as well. This indicates our method can confuse the participants so that they can not distinguish whether it is algorithm-generated or controlled by a real human driver. Thus the proposed is human-like and effective for scene generation for driving intelligence tests. Meanwhile, the accident rate is 14% (most of them are caused by participant 1, rear-end collision), which is higher than usual(Feng et al., 2021), indicating that the participants are actively testing the subject vehicle. This is higher than normal driving but aligns with what we told the drivers before the test: we want them driving normally as a primary task but we also need them to test the subject, which makes our results more reliable. However, there are still some drawbacks in the proposed work as well. One major drawback as reported by the participants is that there are case when driver A acts so indecisive. This is because when the random driving style is too small, the algorithm behaves so cautiously, which does not happen in reality. Also, there is also a overshoot problem for both participants and algorithm. Algorithm overshoot usually happens in the early stage of lane-changing because, as is the same, since the control part is not constrained, when α_{th} is too small, the driver will tries to get away from the obstacle driver. As for real human driver, the overshoot usually happens in the late stage of lane changing because when they accelerate too heavily, they can not control the vehicle properly. On the other hand, these cases are rare. Hence, we think the results is generally valid. In future work, we may take the control level into consideration to generate more human-like behavior. Also, we will increase the number of participants and set a base-line for the test as well.

Conclusion

This paper presents a human-like decision-making algorithm for driving intelligence tests. The interaction model of road users is firstly established using the Bayesian game theory. Besides an extreme conservative choice or an extreme aggressive choice, a probing behavior can be generated using the proposed method based on the cost and relative aggressiveness probability. To evaluate the aggressiveness of the opponent, an observation model is established and the way to customize it is given by an experiment. Additionally, the driver's probing strategy generation method is developed to test the real aggressiveness of the background vehicle. The strategy is reflected on the vehicle's behavior through a proposed Markov method. Next, the proposed methodology is compared with commonly used approaches and state of art literature. The comparison indicates that our method concurs with previous researches while is capable of generating more complex and human-like behavior. Finally, the human-likeness of our algorithm is evaluated using the Turing test. The test results indicate that the participants cannot distinguish human behavior from the behavior generated by our algorithm.

Although the proposed method is designed for scene generation, it may shed some light on the autonomous driving algorithm as well. One of the major challenges in autonomous driving is the uncertainty of traffic. Instead of passively accepting the probability, we may actively make some small steps to reduce the entropy without compromising safety as is given in this paper. Current researches focus on prediction accuracy and learning convergence, which is supposed to be a trade-off between perception/computation burden, and accuracy; the more data available, the more powerful the computer is, the better the decision can be. In this way, we may eventually be able to predict the future, thus obtain a best decision. But, this demand is endless. The decision algorithm, as well as prediction and aggressiveness estimation methodology in this paper, are simple and direct, thus computationally efficient because we do not insist on the global best decision, which is the same for normal human drivers; when human drivers are confused, they just try with small steps, which are simple but powerful.

Additionally, the Turing test framework given in this paper might be applied to autonomous driving algorithm evaluation. As so many researchers and manufacturers are developing human-like self-driving algorithms, this unified and objective method can be used for the assessment of human-likeness.

Our future work will focus on the human control level. Other human behaviors, such as human distraction, control latency will be considered to generate more human-like behavior for autonomous tests. Also, the Markov method will be replaced with a better approximator that can be even more tightly connected to the strategy. Moreover, a more general Turing test procedure with more participants might be our focus as well.

Acknowledgements

This work was supported in part by the SUG-NAP Grant (No. M4082268.050) of Nanyang Technological University, the A*STAR Grant of Singapore (No. 1922500046).

Conflict of interest

The authors declare no competing interests.

Supporting Information

Supporting Information is available from the Wiley Online Library or from the author.

References

Tommaso Colombo, Giulio Panzani, Sergio M. Savaresi, and Pascal Paparo. Absolute driving style estimation for ground vehicles. In *2017 IEEE Conference on Control Technology and Applications (CCTA)*. IEEE, aug 2017. doi: 10.1109/ccta.2017.8062777. URL https://doi.org/10.1109%2Fccta.2017.8062777.

Thomas A. Dingus, Feng Guo, Suzie Lee, Jonathan F. Antin, Miguel Perez, Mindy Buchanan-King, and Jonathan Hankey. Driver crash risk factors and prevalence evaluation using naturalistic driving data. *Proceedings of the National Academy of Sciences*, 113(10):2636–2641, feb 2016. doi: 10.1073/pnas.1513271113. URL https://doi.org/10.1073%2Fpnas.1513271113.

S Feng, X Yan, H Sun, Y Feng, and HX Liu. Intelligent driving intelligence test for autonomous vehicles with naturalistic and adversarial environment. *Nat Commun*, 12:748, Feb 2021.

Lex Fridman, Daniel E. Brown, Michael Glazer, William Angell, Spencer Dodd, Benedikt Jenik, Jack Terwilliger, Aleksandr Patsekin, Julia Kindelsberger, Li Ding, Sean Seaman, Alea Mehler, Andrew Sipperley, Anthony Pettinato, Bobbie D. Seppelt, Linda Angell, Bruce Mehler, and Bryan Reimer. MIT Advanced Vehicle Technology Study: Large-Scale Naturalistic Driving Study of Driver Behavior and Interaction With Automation. *IEEE Access*, 7:102021–102038, 2019. doi: 10.1109/access.2019.2926040. URL https://doi.org/10.1109%2Faccess.2019.2926040.

Kai Gao, Di Yan, Fan Yang, Jin Xie, Li Liu, Ronghua Du, and Naixue Xiong. Conditional Artificial Potential Field-Based Autonomous Vehicle Safety Control with Interference of Lane Changing in Mixed Traffic Scenario. *Sensors*, 19(19):4199, sep 2019. doi: 10.3390/s19194199. URL https://doi.org/10.3390%2Fs19194199.

Peng Hang, Chen Lv, Chao Huang, Jiacheng Cai, Zhongxu Hu, and Yang Xing. An Integrated Framework of Decision Making and Motion Planning for Autonomous Vehicles Considering Social Behaviors. *IEEE Transactions on Vehicular Technology*, 69(12):14458–14469, dec 2020a. doi: 10.1109/tvt.2020.3040398. URL https://doi.org/10.1109%2Ftvt.2020.3040398.

Peng Hang, Chen Lv, Chao Huang, Jiacheng Cai, Zhongxu Hu, and Yang Xing. An Integrated Framework of Decision Making and Motion Planning for Autonomous Vehicles Considering Social Behaviors. *IEEE Transactions on Vehicular Technology*, 2020b.

Peng Hang, Chao Huang, Zhongxu Hu, Yang Xing, and Chen Lv. Decision Making of Connected Automated Vehicles at an Unsignalized Roundabout Considering Personalized Driving Behaviours. *IEEE Transactions on Vehicular Technology*, 70(5):4051–4064, may 2021a. doi: 10.1109/tvt.2021.3072676. URL https://doi.org/10.1109%2Ftvt.2021.3072676.

Peng Hang, Chen Lv, Yang Xing, Chao Huang, and Zhongxu Hu. Human-Like Decision Making for Autonomous Driving: A Noncooperative Game Theoretic Approach. *IEEE Transactions on Intelligent Transportation Systems*, 22(4):2076–2087, apr 2021b. doi: 10.1109/tits.2020.3036984. URL https://doi.org/10.1109%2Ftits.2020.3036984.

Xuemin Hu, Long Chen, Bo Tang, Dongpu Cao, and Haibo He. Dynamic path planning for autonomous driving on various roads with avoidance of static and moving obstacles. *Mechanical Systems and Signal Processing*, 100:482–500, feb 2018. doi: 10.1016/j.ymssp.2017.07.019. URL https://doi.org/10.1016%2Fj.ymssp.2017.07.019.

Zhongxu Hu, Chen Lv, Peng Hang, Chao Huang, and Yang Xing. Data-driven Estimation of Driver Attention using Calibration-free Eye Gaze and Scene Features. *IEEE Transactions on Industrial Electronics*, pages 1–1, 2021a. doi: 10.1109/tie.2021.3057033. URL https://doi.org/10.1109%2Ftie.2021.3057033.

Zhongxu Hu, Yang Xing, Chen Lv, Peng Hang, and Jie Liu. Deep convolutional neural network-based Bernoulli heatmap for head pose estimation. *Neurocomputing*, 436:198–209, may 2021b. doi: 10.1016/j.neucom.2021.01.048. URL https://doi.org/10.1016%2Fj.neucom.2021.01.048.

Chao Huang, Hailong Huang, Peng Hang, Hongbo Gao, Jingda Wu, Zhiyu Huang, and Chen Lv. Personalized Trajectory Planning and Control of Lane-Change Maneuvers for Autonomous Driving. *IEEE Transactions on Vehicular Technology*, 70(6):5511–5523, jun 2021a. doi: 10.1109/tvt.2021.3076473. URL https://doi.org/10.1109%2Ftvt.2021.3076473.

Chao Huang, Chen Lv, Peng Hang, and Yang Xing. Toward Safe and Personalized Autonomous Driving: Decision-Making and Motion Control With DPF and CDT Techniques. *IEEE/ASME Transactions on Mechatronics*, 26(2):611–620, apr 2021b. doi: 10.1109/tmech.2021.3053248. URL https://doi.org/10.1109%2Ftmech.2021.3053248.

Zhiyu Huang, Chen Lv, Yang Xing, and Jingda Wu. Multi-modal Sensor Fusion-Based Deep Neural Network for End-to-end Autonomous Driving with Scene Understanding. *IEEE Sensors Journal*, pages 1–1, 2020. doi: 10.1109/jsen.2020.3003121. URL https://doi.org/10.1109%2Fjsen.2020.3003121.

Arne Kesting, Martin Treiber, and Dirk Helbing. General Lane-Changing Model MOBIL for Car-Following Models. *Transportation Research Record: Journal of the Transportation Research Board*, 1999(1):86–94, jan 2007. doi: 10.3141/1999-10. URL https://doi.org/10.3141%2F1999-10.

B Ravi Kiran, Ibrahim Sobh, Victor Talpaert, Patrick Mannion, Ahmad A. Al Sallab, Senthil Yogamani, and Patrick Perez. Deep Reinforcement Learning for Autonomous Driving: A Survey. *IEEE Transactions on Intelligent Transportation Systems*, pages 1–18, 2021. doi: 10.1109/tits.2021.3054625. URL https://doi.org/10.1109%2Ftits.2021.3054625.

S Kolekar, Winter J de, and D Abbink. Human-like driving behaviour emerges from a risk-based driver model. *Nat Commun*, 11:4850, Sep 2020a.

Sarvesh Kolekar, Joost de Winter, and David Abbink. Which parts of the road guide obstacle avoidance? Quantifying the driver's risk field. *Applied Ergonomics*, 89:103196, nov 2020b. doi: 10.1016/j.apergo.2020.103196. URL https://doi.org/10.1016%2Fj.apergo.2020.103196.

Julian F. P. Kooij, Gwenn Englebienne, and Dariu M. Gavrila. Mixture of Switching Linear Dynamics to Discover Behavior Patterns in Object Tracks. *IEEE Transactions on Pattern Analysis and Machine Intelligence*, 38(2):322–334, feb 2016. doi: 10.1109/tpami.2015.2443801. URL https://doi.org/10.1109%2Ftpami.2015.2443801.

Jonny Kuo, Michael G. Lenné, Megan Mulhall, Tracey Sletten, Clare Anderson, Mark Howard, Shantha Rajaratnam, Michelle Magee, and Allison Collins. Continuous monitoring of visual distraction and drowsiness in shift-workers during naturalistic driving. *Safety Science*, 119:112–116, nov 2019. doi: 10.1016/j.ssci.2018.11.007. URL https://doi.org/10.1016%2Fj.ssci.2018.11.007.

Steven M. LaValle and James J. Kuffner. Randomized Kinodynamic Planning. *The International Journal of Robotics Research*, 20(5):378–400, may 2001. doi: 10.1177/02783640122067453. URL https://doi.org/10.1177%2F02783640122067453.

Andreas Lawitzky, Daniel Althoff, Christoph F. Passenberg, Georg Tanzmeister, Dirk Wollherr, and Martin Buss. Interactive scene prediction for automotive applications. In *2013 IEEE Intelligent Vehicles Symposium (IV)*. IEEE, jun 2013. doi: 10.1109/ivs.2013.6629601. URL https://doi.org/10.1109%2Fivs.2013.6629601.

Liangzhi Li, Kaoru Ota, and Mianxiong Dong. Humanlike Driving: Empirical Decision-Making System for Autonomous Vehicles. *IEEE Transactions on Vehicular Technology*, 67(8):6814–6823, aug 2018. doi: 10.1109/tvt.2018.2822762. URL https://doi.org/10.1109%2Ftvt.2018.2822762.

Nanxiang Li and Carlos Busso. Detecting Drivers' Mirror-Checking Actions and Its Application to Maneuver and Secondary Task Recognition. *IEEE Transactions on Intelligent Transportation Systems*, 17(4):980–992, apr 2016. doi: 10.1109/tits.2015.2493451. URL https://doi.org/10.1109%2Ftits.2015.2493451.

Xiaohan Li, Wenshuo Wang, and Matthias Roetting. Estimating Driver's Lane-Change Intent Considering Driving Style and Contextual Traffic. *IEEE Transactions on Intelligent Transportation Systems*, 20(9):3258–3271, sep 2019. doi: 10.1109/tits.2018.2873595. URL https://doi.org/10.1109%2Ftits.2018.2873595.

Manuel Lindorfer, Christoph F. Mecklenbrauker, and Gerald Ostermayer. Modeling the Imperfect Driver: Incorporating Human Factors in a Microscopic Traffic Model. *IEEE Transactions on Intelligent Transportation Systems*, 19(9):2856–2870, sep 2018. doi: 10.1109/tits.2017.2765694. URL https://doi.org/10.1109%2Ftits.2017.2765694.

Alexander Liniger and John Lygeros. A Noncooperative Game Approach to Autonomous Racing. *IEEE Transactions on Control Systems Technology*, 28(3):884–897, may 2020. doi: 10.1109/tcst.2019.2895282. URL https://doi.org/10.1109%2Ftcst.2019.2895282.

Clara Marina Martinez, Mira Heucke, Fei-Yue Wang, Bo Gao, and Dongpu Cao. Driving Style Recognition for Intelligent Vehicle Control and Advanced Driver Assistance: A Survey. *IEEE Transactions on Intelligent Transportation Systems*, 19(3):666–676, mar 2018. doi: 10.1109/tits.2017.2706978. URL https://doi.org/10.1109%2Ftits.2017.2706978.

Callum Mole, Jami Pekkanen, William E. A. Sheppard, Gustav Markkula, and Richard M. Wilkie. Drivers use active gaze to monitor waypoints during automated driving. *Scientific Reports*, 11(1), jan 2021. doi: 10.1038/s41598-020-80126-2. URL https://doi.org/10.1038%2Fs41598-020-80126-2.

Stephan Muhlbacher-Karrer, Ahmad Haj Mosa, Lisa-Marie Faller, Mouhannad Ali, Raiyan Hamid, Hubert Zangl, and Kyandoghere Kyamakya. A Driver State Detection System—Combining a Capacitive Hand Detection Sensor With Physiological Sensors. *IEEE Transactions on Instrumentation and Measurement*, 66(4):624–636, apr 2017. doi: 10.1109/tim.2016.2640458. URL https://doi.org/10.1109%2Ftim.2016.2640458.

Md Munir, Sarder Fakhrul Abedin, Ki Tae Kim, Do Hyeon Kim, Md Alam, Golam Rabiul, and Choong Seon Hong. Drive Safe: Cognitive-Behavioral Mining for Intelligent Transportation Cyber-Physical System. 2020.

Yadollah Rasekhipour, Amir Khajepour, Shih-Ken Chen, and Bakhtiar Litkouhi. A Potential Field-Based Model Predictive Path-Planning Controller for Autonomous Road Vehicles. *IEEE Transactions on Intelligent Transportation Systems*, 18(5):1255–1267, may 2017. doi: 10.1109/tits.2016.2604240. URL https://doi.org/10.1109%2Ftits.2016.2604240.

Eike Rehder, Jannik Quehl, and Christoph Stiller. Driving like a human: Imitation learning for path planning using convolutional neural networks. *International Conference on Robotics and Automation Workshops*, 2017.

Greg Rupp, Chris Berka, Amir H. Meghdadi, Marija Stevanović Karić, Marc Casillas, Stephanie Smith, Theodore Rosenthal, Kevin McShea, Emily Sones, and Thomas D. Marcotte. EEG-Based Neurocognitive Metrics May Predict Simulated and On-Road Driving Performance in Older Drivers. *Frontiers in Human Neuroscience*, 12, jan 2019. doi: 10.3389/fnhum.2018.00532. URL https://doi.org/10.3389%2Ffnhum.2018.00532.

Dorsa Sadigh, Shankar Sastry, Sanjit A Seshia, and Anca D Dragan. Planning for autonomous cars that leverage effects on human actions. *Robotics: Science and Systems*, 2016.

Kyle Sama, Yoichi Morales, Hailong Liu, Naoki Akai, Alexander Carballo, Eijiro Takeuchi, and Kazuya Takeda. Extracting Human-Like Driving Behaviors From Expert Driver Data Using Deep Learning. *IEEE Transactions on Vehicular Technology*, 69(9):9315–9329, sep 2020. doi: 10.1109/tvt.2020.2980197. URL https://doi.org/10.1109%2Ftvt.2020.2980197.

Jaewook Shin and Myoungho Sunwoo. Vehicle Speed Prediction Using a Markov Chain With Speed Constraints. *IEEE Transactions on Intelligent Transportation Systems*, 20(9):3201–3211, sep 2019. doi: 10.1109/tits.2018.2877785. URL https://doi.org/10.1109%2Ftits.2018.2877785.

Erin T. Solovey, Marin Zec, Enrique Abdon Garcia Perez, Bryan Reimer, and Bruce Mehler. Classifying driver workload using physiological and driving performance data. In *Proceedings of the SIGCHI Conference on Human Factors in Computing Systems*. ACM, apr 2014. doi: 10.1145/2556288.2557068. URL https://doi.org/10.1145%2F2556288.2557068.

Riccardo Spica, Eric Cristofalo, Zijian Wang, Eduardo Montijano, and Mac Schwager. A Real-Time Game

Theoretic Planner for Autonomous Two-Player Drone Racing. *IEEE Transactions on Robotics*, 36(5):1389–1403, oct 2020. doi: 10.1109/tro.2020.2994881. URL https://doi.org/10.1109%2Ftro.2020.2994881.

Mingyu Wang, Zijian Wang, John Talbot, J. Christian Gerdes, and Mac Schwager. Game-Theoretic Planning for Self-Driving Cars in Multivehicle Competitive Scenarios. *IEEE Transactions on Robotics*, 37(4):1313–1325, aug 2021. doi: 10.1109/tro.2020.3047521. URL https://doi.org/10.1109%2Ftro.2020.3047521.

Wenshuo Wang, Junqiang Xi, Alexandre Chong, and Lin Li. Driving Style Classification Using a Semisupervised Support Vector Machine. *IEEE Transactions on Human-Machine Systems*, 47(5):650–660, oct 2017. doi: 10.1109/thms.2017.2736948. URL https://doi.org/10.1109%2Fthms.2017.2736948.

Moritz Werling, Julius Ziegler, Soren Kammel, and Sebastian Thrun. Optimal trajectory generation for dynamic street scenarios in a Fren&#x00E9t Frame. In *2010 IEEE International Conference on Robotics and Automation*. IEEE, may 2010. doi: 10.1109/robot.2010.5509799. URL https://doi.org/10.1109%2Frobot.2010.5509799.

Yang Xing, Chen Lv, Huaji Wang, Dongpu Cao, and Efstathios Velenis. An ensemble deep learning approach for driver lane change intention inference. *Transportation Research Part C: Emerging Technologies*, 115:102615, jun 2020. doi: 10.1016/j.trc.2020.102615. URL https://doi.org/10.1016%2Fj.trc.2020.102615.

Donghao Xu, Zhezhang Ding, Xu He, Huijing Zhao, Mathieu Moze, Francois Aioun, and Franck Guillemard. Learning From Naturalistic Driving Data for Human-Like Autonomous Highway Driving. *IEEE Transactions on Intelligent Transportation Systems*, pages 1–14, 2020. doi: 10.1109/tits.2020.3001131. URL https://doi.org/10.1109%2Ftits.2020.3001131.

Sen Yang, Wenshuo Wang, Fengqi Zhang, Yuhui Hu, and Junqiang Xi. Driving-Style-Oriented Adaptive Equivalent Consumption Minimization Strategies for HEVs. *IEEE Transactions on Vehicular Technology*, 67(10):9249–9261, oct 2018. doi: 10.1109/tvt.2018.2855146. URL https://doi.org/10.1109%2Ftvt.2018.2855146.

Hongtao Yu, H. Eric Tseng, and Reza Langari. A human-like game theory-based controller for automatic lane changing. *Transportation Research Part C: Emerging Technologies*, 88:140–158, mar 2018. doi: 10.1016/j.trc.2018.01.016. URL https://doi.org/10.1016%2Fj.trc.2018.01.016.

Qingyu Zhang, Reza Langari, H. Eric Tseng, Dimitar Filev, Steven Szwabowski, and Serdar Coskun. A Game Theoretic Model Predictive Controller With Aggressiveness Estimation for Mandatory Lane Change. *IEEE Transactions on Intelligent Vehicles*, 5(1):75–89, mar 2020a. doi: 10.1109/tiv.2019.2955367. URL https://doi.org/10.1109%2Ftiv.2019.2955367.

Sumin Zhang, Yongshuai Zhi, Rui He, and Jianping Li. Research on Traffic Vehicle Behavior Prediction Method Based on Game Theory and HMM. *IEEE Access*, 8:30210–30222, 2020b. doi: 10.1109/access.2020.2971705. URL https://doi.org/10.1109%2Faccess.2020.2971705.

Yi Zhang, Ping Sun, Yuhan Yin, Lin Lin, and Xuesong Wang. Human-like Autonomous Vehicle Speed Control by Deep Reinforcement Learning with Double Q-Learning. In *2018 IEEE Intelligent Vehicles Symposium (IV)*. IEEE, jun 2018. doi: 10.1109/ivs.2018.8500630. URL https://doi.org/10.1109%2Fivs.2018.8500630.